energies

Article

Development of a Fault-Diagnosis System through the Power Conversion Module of an Electric Vehicle Fast Charger

Sang-Jun Park [1], Woo-Joong Kim [1], Byeong-Su Kang [1], Sung-Hyun Jang [1], Yeong-Jun Choi [2] and Young-Sun Hong [1,*]

1 Sustainable Technology and Wellness R&D Group, Korea Institute of Industrial Technology, 102 Jejudaehak-ro, Jeju-si 63243, Jeju-do, Korea; psj1949@kitech.re.kr (S.-J.P.); mrkim0403@kitech.re.kr (W.-J.K.); byeongsu88@kitech.re.kr (B.-S.K.); sunghjang@kitech.re.kr (S.-H.J.)
2 Department of Electrical Engineering, Jeju National University, 102 Jejudaehak-ro, Jeju-si 63243, Jeju-do, Korea; yeongjun.choi@jejunu.ac.kr
* Correspondence: yshong@kitech.re.kr; Tel.: +82-64-754-1532; Fax: +82-64-754-1520

Abstract: The supply of electric vehicles (EVs), charging infrastructure, and the demand for chargers are rapidly increasing owing to global low-carbon and eco-friendly policies. As the maintenance of charging infrastructure varies depending on the manufacturer, fault detection and maintenance cannot be conducted promptly. Consequently, user inconvenience increases and becomes an obstacle to EV distribution. Recognizing charger failure after occurrence is a management method that is not economically effective in terms of follow-up. In this study, a data collection system was developed to diagnose EV fast-charger failure remotely in advance. The power module failure-prediction and management system consists of an AC sensor, DC sensor, temperature and humidity sensor, communication board, and data processing device. Furthermore, it was installed inside the fast charger. Four AC inputs, four DC outputs, and temperature and humidity data were collected for 12 months. Using the collected data, the power conversion efficiency was calculated and the power module status was diagnosed. In addition, a multilayer perceptron neural network was used as an algorithm for training the classification model. Charging patterns according to normal and failure were trained and verified. Based on results, the pre-failure diagnosis system demonstrated an accuracy of 97.2%.

Keywords: fast charger; power module; power conversion efficiency; maintenance; diagnostic method; current sensor

Citation: Park, S.-J.; Kim, W.-J.; Kang, B.-S.; Jang, S.-H.; Choi, Y.-J.; Hong, Y.-S. Development of a Fault-Diagnosis System through the Power Conversion Module of an Electric Vehicle Fast Charger. *Energies* **2022**, *15*, 5056. https://doi.org/10.3390/en15145056

Academic Editor: Muhammad Aziz

Received: 16 June 2022
Accepted: 11 July 2022
Published: 11 July 2022

1. Introduction

The supply of electric vehicles (EVs) is expanding owing to the implementation of global eco-friendly and low-carbon policies [1–4]. Accordingly, fast charging and mobile charging infrastructure are rapidly expanding, and improved technology is promptly being developed [5–7]. However, it is difficult to maintain chargers because of several installation points and different maintenance methods owing to the influence of the surrounding environment [8].

For example, economic and time losses are major problems in the fault-detection and maintenance method because it is time consuming to diagnose the fault of the EV charger, prepare the necessary parts, and replace parts. Additionally, it is challenging to generalize and quantify failure types because of the different EV charger manufacturers [9,10]. Consequently, it is difficult to provide charging services to users owing to decreases in the acceptability of EV users and quality of charging services [11,12].

To generalize the main causes of failure in fast chargers, fast charger after-sales service (A/S) history in the Jeju area has been investigated. In particular, causes of failures, such as communication failure, cable failure/damage, display failure, server error, and power module aging, have been investigated. The most frequent A/S maintenance history indicates a decrease in the amount of charge owing to aging of the power module of the fast charger. The power module, as one of the main parts of a fast charger, is expensive and has a short lifespan; therefore, proper management and a pre-failure diagnosis system are required. A fast charger is a combination of four to five submodules with a capacity of 10 to 12.5 kW, and the commonly used charger is a 50 kW-class fast charger [13–15]. If one of these submodules fail, the overall operation is not affected; however, the output is reduced from 50 kW to 40 kW or less, and the charging speed is decreased, resulting in user inconvenience and economic loss. In existing research, equipment and systems for post-inspection of power conversion module failure have been developed; however, in post-inspection, operation efficiency is still a problem, which is caused by not having an appropriate A/S.

To solve this maintenance problem, in this study, a data collection system was established to diagnose the failure of the EV fast charger in advance. In addition, based on the collected data, a system that can remotely diagnose the failure of the power module of a fast charger was developed. Consequently, a system was established that can provide an environment in which the EV charger can be operated economically and efficiently by minimizing the downtime of the charger.

2. Materials and Methods

2.1. Development of Electric Vehicle Fast-Charger Power Module Failure-Prediction and Management System

For the fast charger, the power module failure-prediction and management system was implemented and verified using the JC-9933-TM2KD-3 3 ch 50 kW model of JoongAng Inc. installed in the Wash Zone, Yeonbuk-ro, Jeju Special Self-Governing Province, Korea. The detailed specifications of the fast charger are summarized in Table 1.

Table 1. Detailed specification of fast charger.

EV Fast Charger Specifications			
	Charging method	-	AC (3-phase)/CHAdeMO/CCS TYPE 1
	Input	-	Three-phase, four-wire AC380V, 60 Hz, 50 kVA
	Output	- -	AC: AC380V, 63 A, 40 kW DC: 150~1000 VDC, Max 125 A, 50 kW
	Efficiency/Power Factor	-	95%/0.95
	Environmental conditions	- -	IP54, Temperature: −25~50 °C Humidity: 20~95% (no dew formation)
	Product Certification	-	KC Certification, Type Certification
	Safety functions	-	Overvoltage, overcurrent, undervoltage, leakage current, fusion protection, ground connection

The power module failure-prediction and management system consists of a current sensor (FS9L8, FDS20L1, Fine-trans, Korea), temperature and humidity sensor (CM2305-WP, C-linktech, Korea), communication board (Arduino Due, Arduino, Italia), and data-processing device (Raspberry Pi, Raspberry-Pi, UK). Furthermore, it was installed inside the fast charger, as shown in Figure 1.

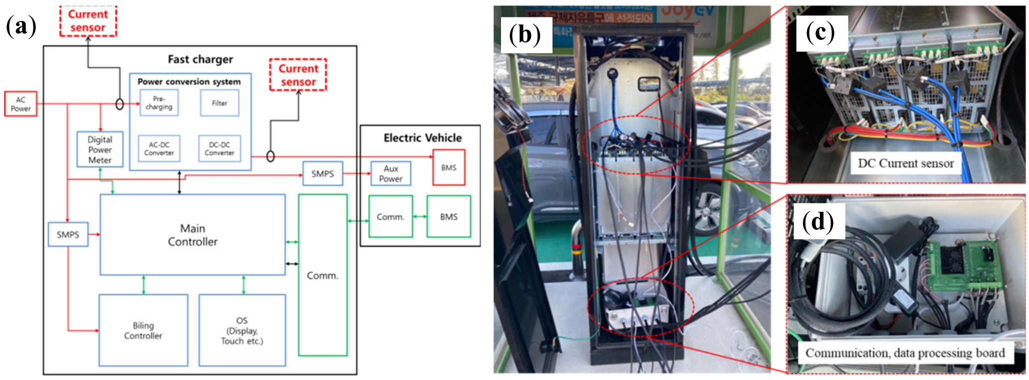

Figure 1. EV fast-charger power module failure-prediction and management system: (**a**) overview; (**b**) overall installation; (**c**) current sensor; (**d**) data-processing board.

By developing a communication protocol for collecting the environmental information of the charger, we developed a system that can provide real-time information such as charging station location, charger type, usage status, power module input/output current, temperature, and humidity. For application to chargers of various manufacturers, we designed and implemented a system for sending and sharing abnormal information data of chargers to the server through a linkable application programming interface (API) format. Table 2 lists the sensor types and main specifications used to develop a fast-charger power module failure-prediction and management system.

Table 2. Detailed specification of fast-charger power module failure-prediction and management system.

Classification	Data Collection Type	Model Name (Manufacturer)	Main Specifications
AC current sensor	Input current (A)	FS9L8 (Fine-trans, Korea)	- Measuring current range: 1~80 A - Measurement accuracy: ±0.1%
DC current sensor	Output current (A)	FDS20L1 (Fine-trans, Korea)	- Measuring current range: 1~70 A - Measurement accuracy: ±0.2%
Temperature/humidity sensor	Temperature, humidity	CM2305-WP (C-linktech, Korea)	- Measuring temperature range: −40~80 °C - Measurement humidity range: 0–99.9% RH - Measurement temperature accuracy: ±0.3 °C - Measurement humidity accuracy: ±2% RH
Communication board	-	Arduino Due (Arduino, Italia)	- Rated Voltage: 3.3~5.5 V - Processor: ARM Cortex-M3
Data processing device	-	Raspberry Pi (Raspberry-Pi, UK)	- Memory: 8 GB - Storage: 32 GB - Operating voltage: 5 V, 3 A

To prevent the server load from transmitting data, a process was established for the fault-diagnosis system to transmit data to the server during charging. When the input current was 1 A or more, the system assessed the operation of the charger, measured the current at the input and output terminals, communicated with the data-processing device, and then transmitted the measured current value. The current, temperature, and humidity data sampling cycle was 1 Hz. In the case of the communication cycle, data recorded for 10 s were transmitted to the server through the communication board.

2.2. Development of Remote Data-Based Fast-Charger Fault-Diagnosis Technology

Fault-diagnosis technology was developed using a fast-charger power module failure-prediction and management system by analyzing the data of 1175 charging times from 17 December 2020 to 10 December 2021. When analyzing the charging pattern, the feature data were selected using the most critical constant current (CC) charging section of the DC output (the section charging 80% of the battery). In addition, the normal and failure data were trained and verified through the test data. By analyzing the charging data, we classified them as follows: a normal charging pattern, charging pattern according to the aging of the power module, and charging pattern according to cable contact failure. A multilayer perceptron (MLP) neural network was used as an algorithm to train the classification model. MLP is an algorithm that enables learning even for data separated into nonlinear regions by placing one or more hidden layers between the input and output layers [16–18]. It learns the data received through the input layer using a number of hidden layers constituting the intermediate stage through several stages, and then derives the predicted value through the output layer [19]. The neural network structure that derives these predicted values is shown in Figure 2 and can be expressed as $\mathrm{f}(\mathrm{x}) = h(3)(h(2)(h(1)(x)))$. The classification results' accuracy was determined according to the charging pattern type through the softmax activation function.

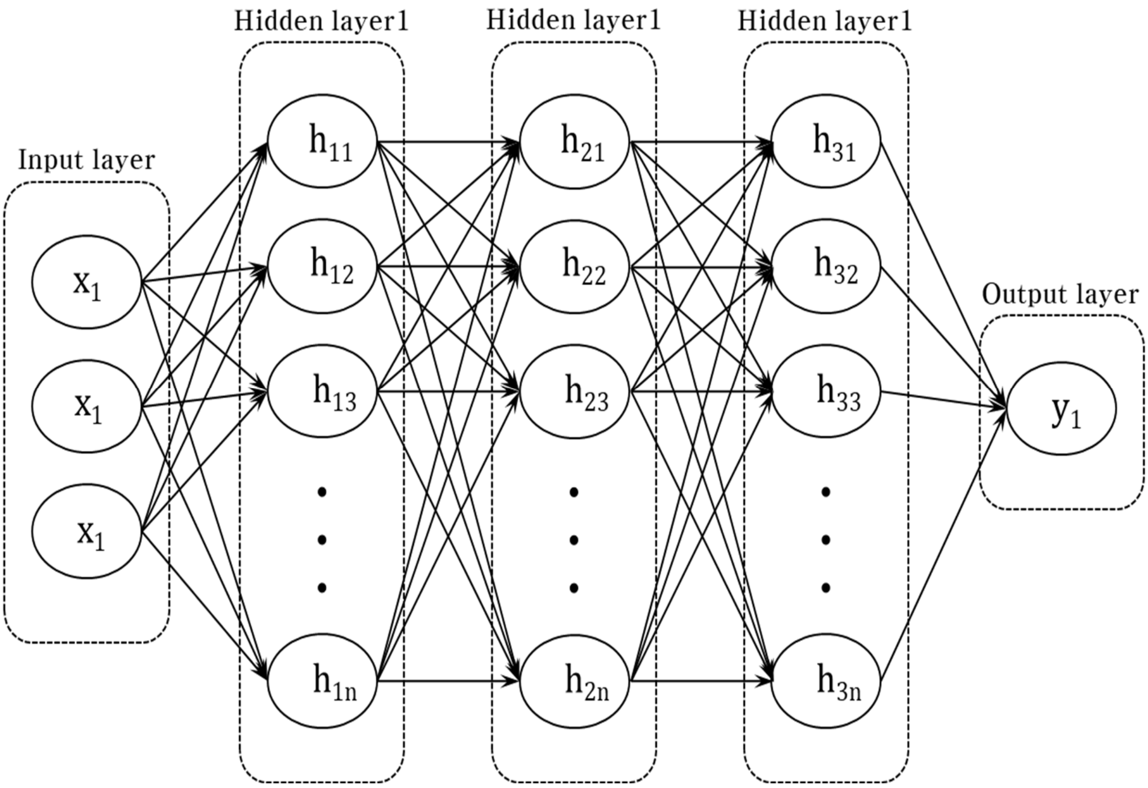

Figure 2. MLP architecture [20].

To analyze the aging of the power module of the fast charger, the power conversion efficiency (PCE) was defined. The PCE is the rate at which the DC output (A) emerges as the AC input (A) enters during rapid charging. The PCE was calculated using Equation (1),

$$\text{PCE} = \text{input current per fast charging/output current per fast charging}, \quad (1)$$

and after judging the aging of the power module according to the numerical value, it was verified through internal analysis.

3. Results and Discussion

For the 50 kW fast charger, the charging pattern of the power module was classified using a pre-failure diagnosis system. The normal charging pattern was measured 1175 times, and Figure 3a shows a representative normal charging pattern. For the output current, it was rapidly charged through CC up to 80% of the battery capacity, and after 1750 s, it was confirmed that the battery was charged up to 100% of the battery capacity through multistage constant current–constant voltage (MCC-CV) for the safety of the battery [21]. The input current was measured with an AC three-phase current and the measurement period was 1 s. Furthermore, the power module aging pattern was measured 13 times, and Figure 3b shows a representative charging pattern due to aging of the power module. Compared to the normal charging pattern, we confirmed that the efficiency of the PCE decreased during charging, resulting in a slope of the output current between the four power modules. Compared with the normal charging pattern, the input current increased with noise and was unstable. Figure 3c shows the charging pattern due to poor contact with the cable of the fast charger. Bad contact charging patterns were observed four times. We confirmed that the output current deviated at the 200 s and 1700 s points owing to poor cable contact.

The PCE of each power module for 300 fast charging cycles through the pre-failure-diagnosis system is shown in Figure 4a–d, which is a linear graph fitting PCE for each power module. The difference in PCE values was caused by the charging profiles of different EVs. However, since there was no significant difference in the PCE values of the four power modules according to one-time charging, an overall trend could be observed. It can be observed that the PCE slope exhibits a downward trend according to the aging of the power module. Figure 4e shows a fitted PCE line graph for each power module. Consequently, we confirmed that the aging of the second power module was more advanced than that of the other power modules.

As the PCE of the No. 2 power module decreases rapidly, the aging progresses. To verify deterioration, as shown in Figure 5, after disassembling No. 2 power module, the interior was observed. Figure 5a shows the front side of the power module, Figure 5b rear side, Figure 5c front heat sink, and Figure 5d rear heat sink. Internal analysis revealed that the heat sink surrounding the switching transistor blackened. We determined that the switching transistor deteriorated because the energy lost during the conversion to DC was released as heat. Accordingly, we confirmed that the PCE of power module of No. 2 decreased. In addition, by checking the output of the fast charger, we confirmed that the output decreased from 50 to 40–42 kW.

The aging of the No. 2 Power Module was confirmed through PCE, and the cause of aging was analyzed and verified through internal analysis. The No. 2 power module was replaced with a new product, and the PCE results are shown in Figure 6. It can be observed that the PCE of No. 1, 3, and 4 power modules decreases after 297 charging cycles, but the PCE of the No. 2 power module increases. This can facilitate the operation of the charger by preventing malfunctions in advance when maintenance is performed by diagnosing the failure and aging of the fast charger through the PCE. This contributes to an increase in the sales of charging station operators by reducing user inconvenience and minimizing downtime.

Classification of Fast-Charger Charging Patterns Using Deep-Learning-Based MLP Algorithm

In the case of a straight line fitted through the PCE, it is accurate to predict the failure and deterioration of the power module of the fast charger in advance and perform maintenance. However, because it is necessary to obtain a graph of a straight line by fitting points of at least 20 to 50, it is difficult to diagnose the failure of the power module of the fast charger with one charge. Accordingly, as shown in Figure 7, after extracting the most critical fast-charging section from the fast charger, four features' data were calculated through data preprocessing, as shown in Table 3.

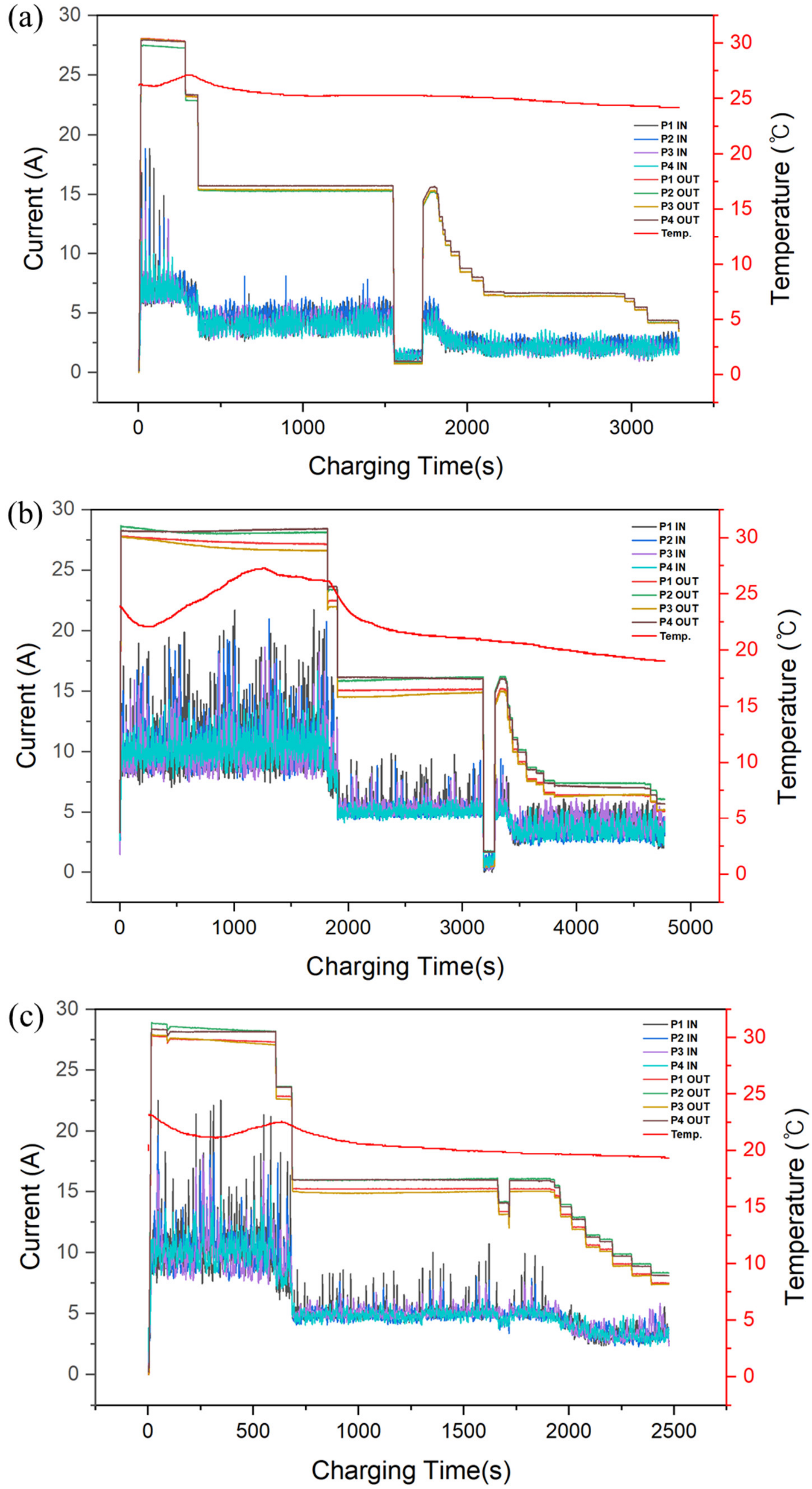

Figure 3. (**a**) Fast-charger normal charging pattern; (**b**) Power-module-aging charging pattern; (**c**) Cable-contact-failure charging pattern. (P1, P2, P3, P4 IN: No. 1, 2, 3, 4 power module input current, P1, P2, P3, P4 OUT: No. 1, 2, 3, 4 power module output current, Temp: Temperature).

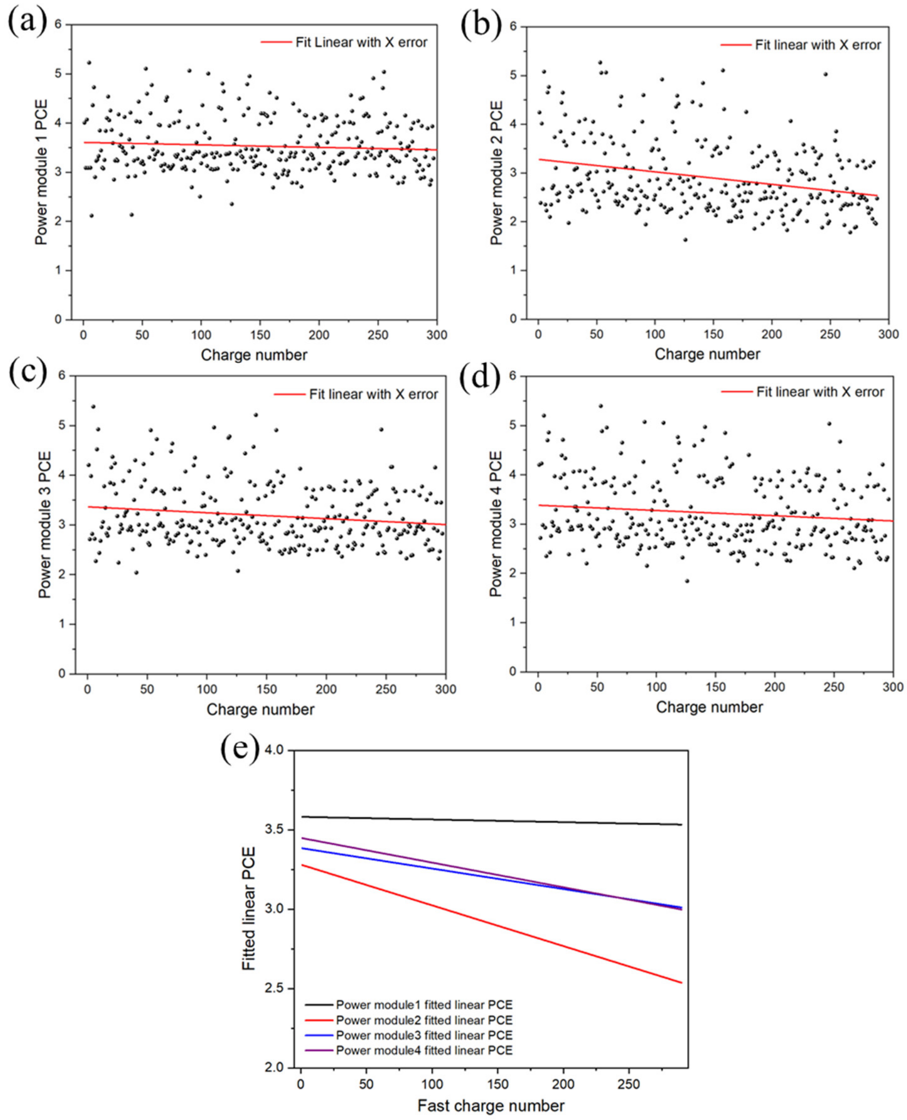

Figure 4. (**a**) No. 1 Power module PCE; (**b**) No. 2 Power module PCE; (**c**) No. 3 Power module PCE (**d**) No. 4 Power module PCE; (**e**) Fitted linear PCE of each power module.

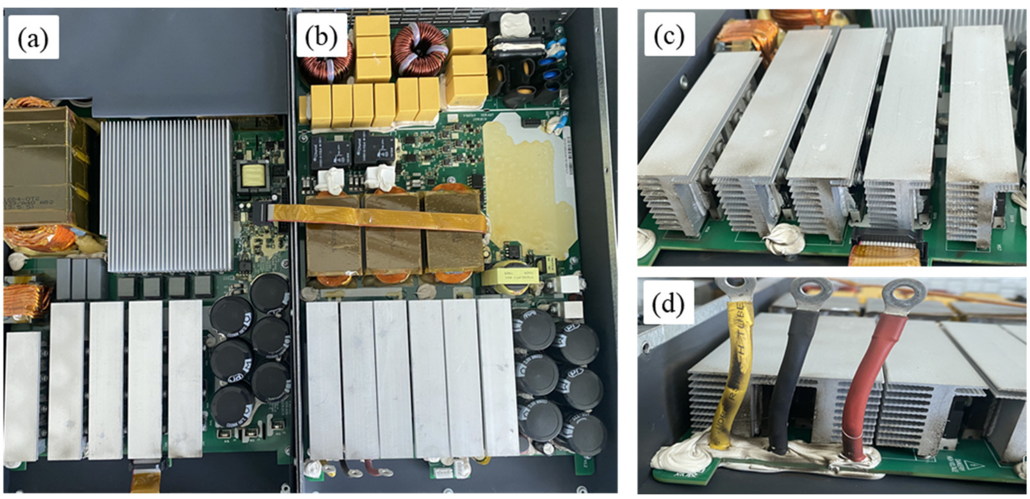

Figure 5. No. 2 power module interior photo after 9 months of use: (**a**) power module front; (**b**) power module rear; (**c**) front heat sink; (**d**) rear heat sink.

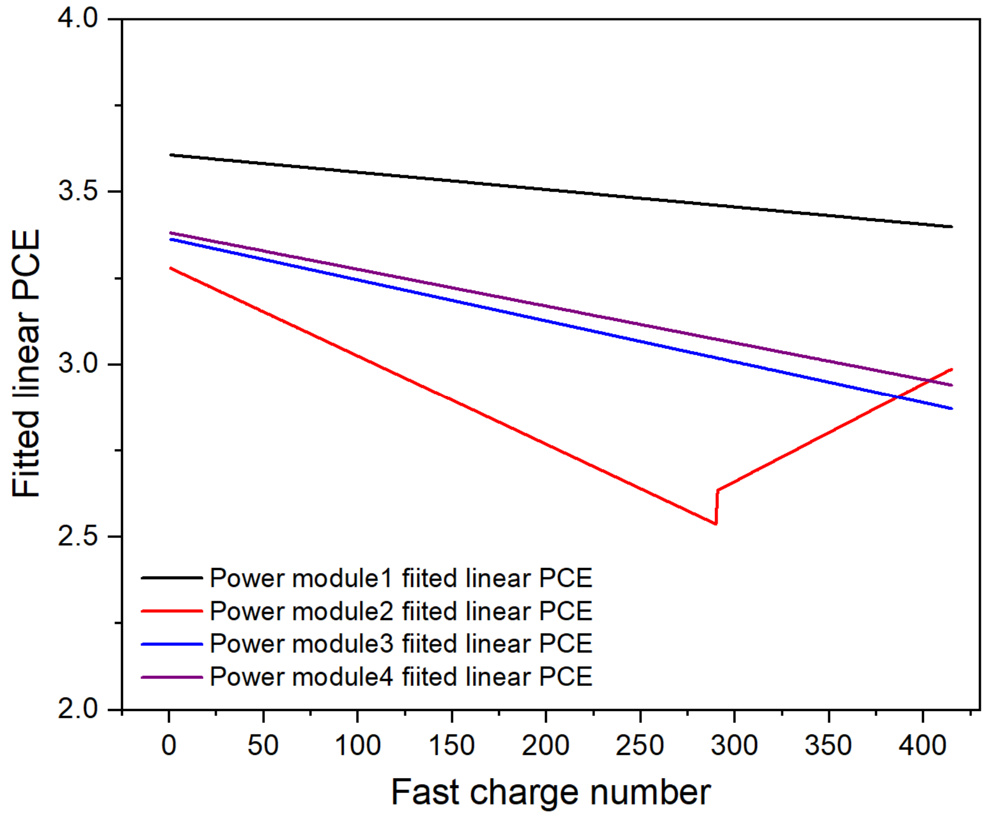

Figure 6. Fitted PCE after replacing No. 2 power module.

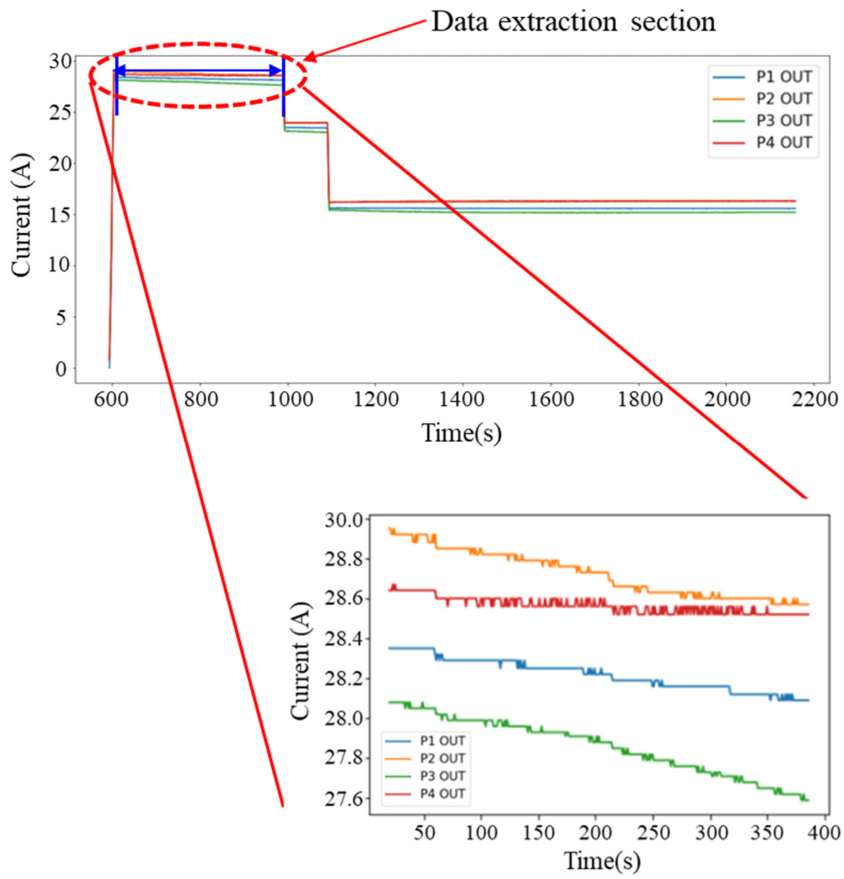

Figure 7. Fast-charger output current (DC) data extraction.

Table 3. Feature data calculation method using analysis section data.

Classification	Feature Data Calculation
Feature 1	Slope MAX–MIN of four power Modules
Feature 2	Average value of slope of four power modules
Feature 3	Slope standard deviation values of four power modules
Feature 4	Number of abnormal signal data

Through feature data, the failure of the fast charger was diagnosed using a deep-learning-based MLP algorithm classification model. A total of 150 training datasets were normalized using 143 normal charging patterns, three power-module-aging charging patterns, and four charging patterns with poor cable contact, and then trained on an MLP-based classification model. The independent variable was designated as four features' data, and the dependent variable was classified into three charging patterns: normal, aging, and poor cable contact. There was a total of six test datasets. Table 4 shows the results of applying the classification model previously using two normal charging patterns, two aging charging patterns for power modules, and two poor cable contacts. From the table, clear characteristics of the feature data are found in the case of normal and poor contact, and the detection results show high accuracies of 98.2% and 97.9%, respectively. In the case of the aging data, the number of training data is relatively small, and a classification accuracy of 95.4% can be obtained because it is not clearly distinguished from the normal data. The power module aging data were previously confirmed as the data of the second power module, and were classified as a normal charging pattern after replacement with a new power module. The learning model developed in this study classifies charging patterns with high accuracy using only one charging. Therefore, if a pre-failure diagnosis system is installed in the manufacturing process of a rapid charger, it will be possible to effectively save time while maintaining the charger by minimizing its idle time.

Table 4. Classification accuracy by type of fast-charging pattern.

Charging Pattern	Number of Training Data	Number of Validation Data	Classification Accuracy Charging Pattern (%)
Normal charging pattern	143	2	98.2
Power-module-aging charging pattern	3	2	95.4
Poor-cable-contact charging pattern	4	2	97.9
Average			97.2

4. Conclusions

In this study, a preliminary fault-diagnosis system for fast chargers was developed and then applied to a quick charger at the Wash Zone branch in Jeju Special Self-Governing Province. Using the collected data, the PCE was calculated and the status of the power module was diagnosed. According to the PCE data analysis for a total of nine months, the fitted linear PCE of the No. 2 power module significantly decreased compared to other power modules. Accordingly, the No. 2 power module was disassembled and an internal analysis was performed. We confirmed that the PCE of the No. 2 power module after 297 charging cycles was reduced owing to the aging of the switching transistor. According to the PCE analysis for the remaining three months after replacing the No. 2 power module with a new one, the PCE showed a tendency to increase compared to the other power modules. In addition, we confirmed that the PCE in the No. 2 power module has a higher value than those of the existing No. 3 and 4 power modules, which verified the aging of the No. 2 power module. To diagnose the failure of the fast charger with only one fast charge, the critical section was extracted during fast charging, corresponding feature data were calculated, and failure of the fast charger was diagnosed using a deep-learning-based MLP algorithm classification model. The classification accuracy according to the aging of the power module was 95.4%, normal charging pattern classification was 98.2%, and charging pattern classification was 97.9% owing to poor cable contact. In this study, a prototype system was developed for pre-failure diagnosis of fast chargers. If the proposed fast-charger pre-failure-diagnosis system is added to the fast-charger manufacturing process after increasing its accuracy and reliability through weight reduction and deep AI learning, it can help systematize maintenance, increase sales of the charger operating office, and increase the sales to users of electric vehicle. In addition, it will contribute to the expansion of EV distribution by improving convenience.

Author Contributions: Conceptualization, S.-J.P. and Y.-S.H.; methodology, B.-S.K.; software, S.-H.J.; validation, Y.-S.H., S.-J.P. and W.-J.K.; formal analysis, Y.-J.C.; investigation, W.-J.K.; resources, Y.-S.H.; data curation, S.-J.P.; writing—original draft preparation, S.-J.P.; writing—review and editing, Y.-S.H.; visualization, B.-S.K.; supervision, Y.-S.H.; project administration, B.-S.K.; funding acquisition, Y.-S.H. All authors have read and agreed to the published version of the manuscript.

Funding: This work was supported by the Korea Ministry of Trade, Industry, and Energy (MOTIE), under the grant "Implementation of on-board grade estimation for EV battery using database and verifying re-use applications with used batteries (No. P0021883)".

Institutional Review Board Statement: Not applicable.

Informed Consent Statement: Not applicable.

Data Availability Statement: Not applicable.

Conflicts of Interest: The authors declare no conflict of interest.

References

1. Pallonetto, F.; Galvani, M.; Torti, A.; Vantini, S. A framework for analysis and expansion of public charging infrastructure under fast penetration of electric vehicles. *World Electr. Veh. J.* **2020**, *11*, 18. [CrossRef]
2. Suarez, C.; Martinez, W. Fast and ultra-fast charging for battery electric vehicles–A review. In Proceedings of the 2019 IEEE Energy Conversion Congress and Exposition (ECCE), Baltimore, MD, USA, 29 September–3 October 2019; pp. 569–575. [CrossRef]
3. De Quevedo, P.M.; Muñoz-Delgado, G.; Contreras, J. Impact of electric vehicles on the expansion planning of distribution systems considering renewable energy, storage, and charging stations. *IEEE Trans. Smart Grid.* **2019**, *10*, 794–804. [CrossRef]
4. Wu, Y.A.; Ng, A.W.; Yu, Z.; Huang, J.; Meng, K.; Dong, Z.Y. A review of evolutionary policy incentives for sustainable development of electric vehicles in China: Strategic implications. *Energy Policy* **2021**, *148*, 111983. [CrossRef]
5. Afshar, S.; Macedo, P.; Mohamed, F.; Disfani, V. A literature review on mobile charging station technology for electric vehicles. In Proceedings of the 2020 IEEE Transportation Electrification Conference & Expo (ITEC), Chicago, IL, USA, 23–26 June 2020; pp. 1184–1190. [CrossRef]
6. Morrissey, P.; Weldon, P.; O'Mahony, M. Future standard and fast charging infrastructure planning: An analysis of electric vehicle charging behaviour. *Energy Policy* **2016**, *89*, 257–270. [CrossRef]
7. Viana, C.; Lehn, P.W. A drivetrain integrated DC fast charger with buck and boost functionality and simultaneous drive/charge capability. *IEEE Trans. Transp. Electrif.* **2019**, *5*, 903–911. [CrossRef]
8. Fang, X.; Li, J.; Zhang, X.; Chen, W.; Wang, W. Study on Temperature Control Design and High Protection of Charger. In Proceedings of the 2018 10th International Conference on Intelligent Human-Machine Systems and Cybernetics (IHMSC), Hangzhou, China, 25–26 August 2018; pp. 216–219. [CrossRef]
9. Alavi, S.M.M.; Fekriasl, S.; Niyakan, S.N.; Saif, M. Fault detection and isolation in batteries power electronics and chargers. *J. Energy Storage* **2019**, *25*, 100807. [CrossRef]
10. Chen, W.; Wang, L.; Ulatowski, A.; Bazzi, A.M. A fuzzy logic approach for fault diagnosis and recovery in PHEV and EV chargers. In Proceedings of the 2014 IEEE Transportation Electrification Conference and Expo (ITEC), Dearborn, MI, USA, 15–18 June 2014; pp. 1–5. [CrossRef]
11. Yan, Q.; Dong, H.; Zhang, M. Service evaluation of electric vehicle charging station: An application of improved matter-element extension method. *Sustainability* **2021**, *13*, 7910. [CrossRef]
12. Zhang, L.; Zhao, Z.; Yang, M.; Li, S. A multi-criteria decision method for performance evaluation of public charging service quality. *Energy* **2020**, *195*, 116958. [CrossRef]
13. Chaurasiya, S.; Mishra, N.; Singh, B. A 50kW bidirectional fast EV charger with G2V & V2G/V2V capability and wide voltage range. In Proceedings of the 2020 IEEE 5th International Conference on Computing Communication and Automation (ICCCA), Greater Noida, India, 30–31 October 2020; pp. 652–657. [CrossRef]

14. Kuperman, A.; Levy, U.; Goren, J.; Zafranski, A.; Savernin, A.; Peled, I. Modeling and control of a 50KW electric vehicle fast charger. In Proceedings of the 2010 IEEE 26th Convention of Electrical and Electronics Engineers, Eilat, Israel, 17–20 November 2010; pp. 188–192. [CrossRef]
15. Yoon, H.; Kim, J.; Song, E. Design of a novel 50 kW fast charger for electric vehicles. *J. Cent. South Univ.* **2013**, *20*, 372–377. [CrossRef]
16. Gardner, M.W.; Dorling, S.R. Artificial neural networks (the multilayer perceptron)—a review of applications in the atmospheric sciences. *Atmos. Environ.* **1998**, *32*, 2627–2636. [CrossRef]
17. Heidari, A.A.; Faris, H.; Mirjalili, S.; Aljarah, I.; Mafarja, M. Ant lion optimizer: Theory, literature review, and application in multi-layer perceptron neural networks. In *Nature-Inspired Optimizers. Studies in Computational Intelligence*; Mirjalili, S., Song Dong, J., Lewis, A., Eds.; Springer: Cham, Switzerland, 2020; Volume 811. [CrossRef]
18. Lee, S.; Choeh, J.Y. Predicting the helpfulness of online reviews using multilayer perceptron neural networks. *Expert Syst. Appl.* **2014**, *41*, 3041–3046. [CrossRef]
19. Belue, L.M.; Bauer, K.W. Determining input features for multilayer perceptrons. *Neurocomputing* **1995**, *7*, 111–121. [CrossRef]
20. Baum, E.B. On the capabilities of multilayer perceptrons. *J. Complex.* **1988**, *4*, 193–215. [CrossRef]
21. Li, S.; Zhang, C.; Xie, S. Research on fast charge method for lead-acid electric vehicle batteries. In Proceedings of the 2009 International Workshop on Intelligent Systems and Applications, Wuhan, China, 23–24 May 2009; pp. 1–5. [CrossRef]